Received 1 July 2024; revised 28 July 2024; accepted 20 August 2024. Date of publication 28 August 2024; date of current version 9 September 2024.

Digital Object Identifier 10.1109/OJCOMS.2024.3450809

Weighted Antenna's Azimuth for Minimal EMF With Sustainable KPIs of Multi-Technology BS

MOHAMMED S. ELBASHEIR (Senior Member, IEEE), RASHID A. SAEED (Senior Member, IEEE), AND SALAHELDIN EDAM

School of Electronic Engineering, College of Engineering, Sudan University of Science and Technology, Khartoum 14413, Sudan

CORRESPONDING AUTHOR: M. S. ELBASHEIR (e-mail: mohd.suleiman@gmail.com)

ABSTRACT Nowadays, significant developments in wireless technologies and solutions have led to the rapid expansion of mobile networks, and it's expected to grow more, particularly with the launch of the Fifth Generation New Radio (5G NR). The deployment of a large number of base stations (BSs) is raising concerns about the potential for increased exposure to electromagnetic field radiation (EMF). Many international and national regulators have set guidelines and regulations to control the amount of EMF radiation. This paper presents a design model to de-concentrate the total exposure from sectorized antennas of the multi-technology base station with no drawback on network coverage level and key performance indicators (KPIs). The model applies the concept of weighted antenna's azimuth to spread the total exposure by horizontally separating the installed antennas in the same sector. A set of simulations is conducted to calculate the reduction in total exposure ratio (TER) for widely used setups in antenna deployment for multi-technology mobile networks. Additionally, A field test was done in a life network to evaluate the proposed model in the geographical cluster, and a set of field measurements was conducted to assess the TER and the compliance distance (CD) before and after the test implementation. Further, the operation support system (OSS) records and counters were analyzed to evaluate the impact on the network coverage and capacity behavior, especially for the carried traffic and number of users. The pre-and-post results show that the TER and CD are improved by a valuable reduction after applying the proposed model. Overall, the system records show no significant impacts were registered on network coverage level and capacity performance for all transmitting technologies of the sites involved in the test.

INDEX TERMS Mobile wireless network, antenna sectorization, coverage and capacity planning, EMF compliance distance.

I. INTRODUCTION

MOBILE wireless networks are developing quickly and undergoing massive installations, resulting in an increase in the quantity of transmitting BSs afterward. To give the network enough coverage and increase resource capacity, a huge number of site BSs have been integrated, this has resulted in very large data communications across mobile wireless networks, which will reach considerably greater numbers by 2030 [1], [2]. 2G Global System for Mobile Communication (GSM), 3G Universal Mobile Telecommunications System (UMTS), 4G Long-Term Evolution (LTE), and most recently, 5G NR, are the most widely used technologies in mobile wireless networks. Concerns regarding the negative effects on human health are addressed due to the rise in electromagnetic fields as a result of the development of new technologies [3], [4], [5].

According to predictions, 5G technology will become an all-purpose system [5] since it offers high capacity and makes several features and services possible that increase the number of commercial opportunities and boost the world economy. Installing NR BSs at higher frequency bands is necessary for 5G development [6], mostly by collocating them with existing 2G/3G/4G technologies.

A set of technologies and solutions at one location necessitates an analysis to determine the exposure level referenced to standard limits and to analyze the total accumulated radiation [7], [8], [9]. Many studies indicate this evaluation should take place during the design stage of

the network prior to the deployment as EMF is a constraint in network planning especially for 5G [10], [11].

Almost, all cellular network operators use sectorized BSs with directional antennas, especially the three-sector model that helps to maximize the outdoor and indoor coverage, load balancing, capacity resources management, and interference optimization. Furthermore, the same sectors carry different technologies radiating in the same directions as co-located. Depending on the design strategy of the operator, the group of technologies either be connected to one multi-band antenna, or might be installed into separate antennas, but all antennas of one sector are usually directed in the same azimuth.

The investigation of EMF for multiple technologies is a crucial topic that aims to enhance the assessment of the compliance distance and to introduce models for minimizing it, especially since it requires the operators to identify the compliance distances and mark them as exclusive zones which should be not accessible for the general public.

This work's originality lies in providing a simple model (design technique) to de-concentrate the total exposure emitting from sectorized antennas of the multi-technology BS, while maintaining the network performance with no impact on the coverage signal levels and main KPIs. Additionally, this model can be practically applied to the widely commonly used antennas that are currently installed for multi-technology BS.

This manuscript is structured into seven sections including the introduction in Section I. In Section II, the total exposure ratios in the standard limits are briefed. The literature review and related work are discussed in Section III. In Section IV, the proposed model is explained in detail. In Section V, the CD formula is presented. In Section VI, the simulation setup and results are presented and discussed. In Section VII, the in-situ assessment is explained in detail and the results are discussed. Section VIII discusses the application of the proposed model. At last, Section IX summarizes the paper's conclusion.

II. TOTAL EXPOSURE RATIO AND STANDARD LIMITS

The Federal Communication Commission (FCC) establishes regulatory criteria in the USA [12] and the International Commission on Non-Ionizing Radiation Protection (ICNIRP) established in Europe [13], [14] are two well-known organizations that have set and published standard recommendations for EMF exposure. Governmental and national authorities in many nations have utilized these guidelines to manage the installation of EMF transmitters and the activities associated with them [15], [16], [17], [18]. The FCC and ICNIRP standards make a distinction between the technical occupational workers (OW) and the general public (GP). The OW refers to the staff members who are well-trained to be aware of potential EMF hazards and are exposed to certain related scenarios, and the GP are characterized as being normal people who are exposed to electromagnetic fields and are not aware of the dangers associated with them.

TABLE 1. ICNIRP reference limits for OW and GP.

Exposure Boundary	Frequency Range	E - field (V/m)	H - field (A/m)	P_D (W/m^2)
OW	0.1 - 30MHz	$660/f_M^{0.7}$	$4.9/f_M$	*NA*
	>30 - 400MHz	*61.0*	*0.16*	*10.00*
	>400 - 2,000MHz	$3f_M^{0.5}$	$0.008f_M^{0.5}$	$f_M/40$
	>2.0 - 300GHz	*N/A*	*N/A*	*50.00*
GP	0.1 - 30MHz	$300/f_M^{0.7}$	$2.2/f_M$	*NA*
	>30 - 400MHz	*27.70*	*0.073*	*2.00*
	>400 - 2,000MHz	$1.375f_M^{0.5}$	$0.0037f_M^{0-5}$	$f_M/200$
	>2.0 - 300GHz	*N/A*	*N/A*	*10.00*

TABLE 2. FCC exposure limits for, for OW and GP.

Exposure Boundary	Frequency Range	E - field (V/m)	H - field (A/m)	P_D (W/m^2)
OW	0.3-3.0MHz	*614.0*	*1.630*	*100.0*
	3.0-30 MHz	*1842/f*	*4.89/f*	*900/f^2*
	30-300 MHz	*61.40*	*0.163*	*1.00*
	0.3-1.5GHZ	-	-	*f/300*
	1.5-100GHz	-	-	*5.00*
GP	0.3-1.34 MHz	*614.0*	*1.630*	*100*
	1.34-30 MHz	*824/f*	*2.19/f*	*180/f^2*
	30-300 MHz	*27.50*	*0.0730*	*0.20*
	0.3-1.5GHz	-	-	*f/1500*
	1.5-100GHz	-	-	*1.00*

The whole-body radiation reference levels have been set by ICNIRP for both the occupational workers and the normal general public under the transmitting frequency, as listed in Table 1.

Also, the FCC standard [12] has defined the maximum limits of exposure as the maximum permitted exposure (MPE) levels for the GP and OW according to the transmitting frequency band as listed in Table 2.

III. RELATED WORK AND LITERATURE REVIEW

Owing to the significance of this subject, numerous studies and research projects have been completed, and more are being worked on. Plenty of published results were explored in international organizations, the authors examined the subject from a variety of perspectives and multiple angles, but they all shared the goal of looking into the EMF exposure investigation and assessment.

This section evaluated some examples that were recently published, by exploring their work methods, conclusions, and outcomes. The following summaries are for those works that focused on determining the total exposure and compliance boundaries:

- The authors of [19] suggested conservative formulae to calculate the whole-body and localized SAR for the main beam exposure from the BS. The heuristic nature of the proposed formulas, their applicability to a class of typical base station antennas, their creation from multiple physical observations, and the results of a comprehensive literature review, measurements, and

numerical simulations of typical exposure scenarios all lend support to their creation.

- The compliance distance for 2G GSM operating at 1800 MHz was calculated by the authors in [20] based on field measurements they conducted in various locations within the university (Symbiosis International University campus Pune, India). The calculated compliance distance is 8.4 meters.
- A novel technique for measuring 5G NR exposure based on user actions, including the evaluation of auto-included exposure of base stations and user phones, was suggested by the authors in [21]. Their study is based on information from earlier RF-EMF exposure research as well as certain studies that simulate NR base stations and readings close to test sites.
- In [22], the authors measured the 4G LTE TDD mMIMO in-situ while accounting for 100% traffic load and maximum system utilization. The findings indicate that the EMF level was between 7.3 and 16.1% of the ICNIRP occupational reference level, as opposed to 79.3% based on traditional conservative calculations, and that the actual compliance boundaries were reduced by 2.2–3.3 times the conservatively calculated boundaries. The authors explain this drop by pointing to the irregular and unique conduct of mMIMO beamforming. They also point out that a further fall in the compliance barrier is anticipated because actual RBS traffic loading is typically substantially lower than 100%.
- Pinchera et al. analyzed the power levels surrounding the 5G antenna array in [23] to determine the compliance boundary and appropriately evaluate the exposure level. Using a statistical method, the authors presented a measure called normalized average power pattern (NAPP) for determining the average power density surrounding the antenna. Their findings illustrate the compliance distances that were computed using various power reduction factor values.
- Thielens et al. (at Ghent University) used finite-difference time-domain (FDTD) simulations for a 4G LTE base station antenna at 2,600 MHz in [24] to establish the EMF exposure compliance bounds. Their findings demonstrate that when the antenna is only partially radiating, the reference levels are not conservative for the different fundamental limitations and reference levels. Furthermore, their findings demonstrate that the compliance boundaries for fundamental restrictions at lower antenna powers are provided by the 10g averaged SAR in the head and trunk of the body.
- In [25], Héliot et al. used a commercial 5G BS operating at 3.6 GHz and a mMIMO customizable testbed operating at 2.6 GHz to examine the nature of mMIMO exposure and its effects on the compliance boundary. Their statistical exposure-based exclusive zone definition results are intriguing. According to their investigation, there are considerable changes in exposure depending on the direction of the beams.

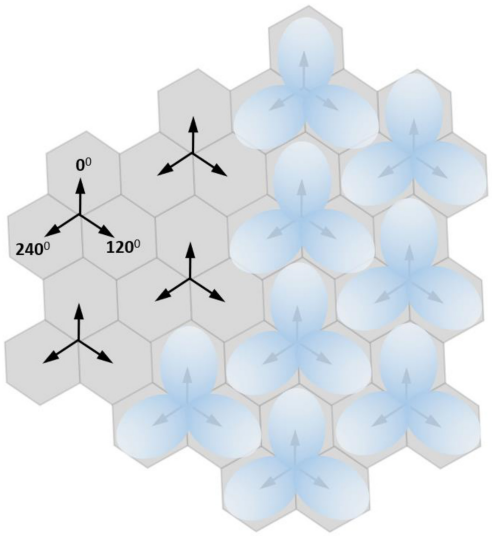

FIGURE 1. The three-sector model with 0/120/240 degrees that commonly used in mobile networks.

Additionally, assuming a fixed traffic load, the variance of exposure tends to decrease as the number of users increases. Conversely, regardless of the user numbers, the exposure rises sub-linearly with traffic load.

IV. TER DE-CONCENTRATION FOR SECTORIZED BS

More effective coverage planning is possible when the site coverage is divided into cell sectors, which means dividing the coverage area into smaller sectors served by individual antennas. RF engineers adjust the signal propagation to reflect the geographic distribution of mobile users by concentrating the coverage in particular directions as shown in Fig. 1 which represents (as an example) the three-sector model with 0/120/240 degrees as antennas' azimuth for the horizontal directions. Within the same cell site, the available frequency spectrum can be utilized numerous times with sectors remaining unaffected. This expands the cell site's total capacity and enables the simultaneous service of additional customers [26]. Also, improved load distribution throughout the cell site is made possible by antenna sectorization. Traffic can be dynamically forwarded across sectors during high usage periods to reduce congestion and guarantee that all users receive sufficient service quality. The RF engineers may simplify their planning and deployment process according to the area's nature, and they focus on improving every region separately, accounting for variables like topography, population density, and anticipated traffic patterns. Generally, sectorization is a commonly used technique in the construction and optimization of mobile cellular networks because it offers a balance between coverage, capacity, and interference control overall [27].

While sectorization can enhance network performance and capacity, it increases the EMF radiation by concentrating the transmitting signals from all technologies in the antenna's direction. Upon the guidelines of ICNIRP and FCC, the total

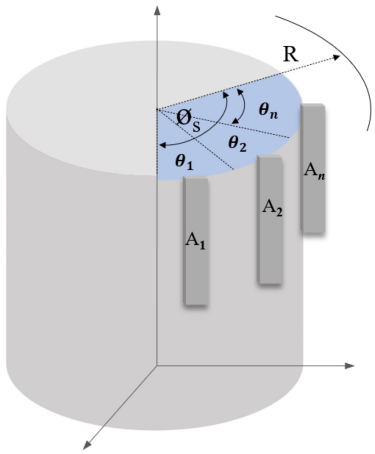

FIGURE 2. One sector with n number of antennas.

exposure should be calculated considering the accumulated power density S in watt/m^2 [12], [13] from the transmitting multi-technology sources.

Fig. 2 shows a sectorized cell with N number of antennas in one sector. From [12], [13], [14] the exposure ratio for each transmitter can be calculated using Equation (1).

$$ER_f = \frac{S_{inc,f}}{S_{inc,RL,f}} \tag{1}$$

where ER_f is the Exposure Ratio at distance R from the transmitting signal at frequency f. $S_{inc,f}$ and $S_{inc,RL,f}$ are the incident local power densities and their reference level at frequency f listed in Tables 1 and 2.

The $S_{inc,f}$ can be calculated using Equation (2):

$$S_{inc,f} = \frac{P_{T,f} \ .G_{A,f}}{4.\pi.R^2} \tag{2}$$

where P_T is the transmitted power in watts, and G_A is the antenna's gain of the transmitter at frequency f.

By substituting Equation (2) in the nominator of Equation (1) it gives Equation (3) as:

$$ER_f = \frac{P_{T,f} \ .G_{A,f}}{4.\pi.R^2.S_{inc,RL,f}} \tag{3}$$

As per [6], [7], [8] the total exposure ratio of all transmitters in antenna n (TER_n) can be calculated using Equation (4):

$$TER_n = \sum_{n,f} ER_f \tag{4}$$

Furthermore, the total exposure ratio of one sector TER_N can be calculated using Equation (5) as:

$$TER_N = \sum_{n=1}^{N} TER_n \tag{5}$$

Thus, by substituting Equation (4) in Equation (5), the TER_N can be calculated using Equation (6) as:

$$TER_N = \sum_{n=1}^{N} \sum_{n,f} ER_f \tag{6}$$

Although the three-sector model is commonly used for cell sectorization, this study considers the general case of Ns number of sectors at one BS in the proposed model. Assuming each sector contributes equally in the TER of one BS, thus, the total exposure of one sector comes through angle width $\varnothing_s$ which can be calculated simply using Equation (7)

$$\varnothing_s = \frac{360}{N_s} \tag{7}$$

Within one sector, the total exposure TER_N can be distributed among the whole $\varnothing_s$ by azimuth shifting the direction of each antenna towered separate sub-angle, each sub-angle has an angle width θ_n where n is the number of antennas in one sector. Each θ_n has an angle value based on the TER_n weight out of the TER_N, which means the θ_n is the weighted angle proportional to TER_n. Of course, this manner is applied for other sectors in the same site to have repeated antenna's azimuth arrangement in the way for one technology to have the same antenna angle separation between all sectors. Thus, this approach gives a model to deconcentrate the total exposure (as spreading) in sub-directions rather than having all antennas transmitting toward one direction. So, the θ_n can be calculated using Equation (8).

$$\theta_n = \varnothing_s * \frac{TER_n}{TER_N} = \frac{360}{N_s} * \frac{TER_n}{TER_N} \tag{8}$$

Finally, by substituting Equations (3), (4), (6) into Equation (8), it gives Equation (9) to calculate the θ_n

$$\theta_n = \frac{360}{N_s} * \sum_{n,f} \frac{P_{T,f} \ .G_{A,f}}{S_{inc,RL,f}} / \left(\sum_{n=1}^{N} \sum_{n,f} \frac{P_{T,f} \ .G_{A,f}}{S_{inc,RL,f}} \right) \tag{9}$$

In life networks, the RF planning engineers determine the antenna's setup including azimuth angles for different technologies depending on many design factors, including target coverage area, frequency planning, capacity distribution, interface control, etc...

The Mobile Network Operators (MNOs) target to provide enough capacity and continuous coverage inside urban and dense areas (cities, and towns) to capture the offered traffic from populated areas. The MNOs deploy the antenna sectorization model with a repeated pattern that uses site-to-site distance to provide continuous coverage. The three-sector model with 0/120/240 degrees is commonly used, and the MNOs apply the same angles for all technologies although each technology has separate dedicated resources and is operating in different frequencies, and functioning separately. The reasons behind using the same azimuth angles for all technologies are the installation simplicity, sometimes using one antenna (multi-band antenna) for different technologies, and enabling maximum traffic balancing between different layers. However, it's not mandatory to use the same azimuth

angles for different technologies as there is continuous coverage which is also which enables traffic balance and control between different technologies.

The proposed solution of applying separation angles between different technologies is advantageous and assists in reducing compliance distances without affecting network performance or coverage, especially inside cities and towns with continuous coverage. The results of this study show applying adjustments to the antenna orientations de-concentrates the total exposure and gives shortened compliance distances for the necessary cases, particularly for wall-mounted and rooftop sites where the antennas are usually placed close to accessible areas.

In the assessment section (Section VII), will discuss in detail the results that show this model doesn't affect the base station performance in terms of coverage level and capacity. However, it is important to mention this model is applicable for macro sites that serve in areas where continuous coverage is required around the whole site area, and it's not applicable for below such cases:

- For sites that have sector's azimuths intentionally are directed toward certain locations for special coverage and capacity requirements such as highway road sites.
- For sites that use one antenna for all technologies such as penta-band and hexa-band antennas.

V. CD FOR SECTORIZED BASE STATION

In [17], [25], the IEC62232 has stated in their guidelines the most precise compliance border possible as an iso surface pattern that may be contained in simpler shaped volume to create more restricting parameters, such as the box-shape (horizontal, vertical, and side) that is appropriate for the sectorized site with the vertical and horizontal boundaries of the coverage antenna. The side CD (R_{CD-S}) can reach maximum value equal to horizontal CD when rotate the antenna's main beams horizontally toward the side direction note that horizontal azimuth can be from 0 to 360 degrees. In this work, the two primary directions facing the horizontal and vertical beams of the antenna are considered similar to related studies found in the [19], [20], [28], [29], [30] assuming the R_{CD-H} is maximum boundary for all horizonal directions including side direction as shown in Fig. 3.A and Fig. 3.B the R_{CD} is the compliance distance in the two directions (R_{CD-H} at the horizontal, and R_{CD-V} at vertical) from the transmitter at which the entire *TER* equals one as per ICNIRP and FCC guidelines [12], [13], [14].

The R_{CD}, where $TER = 1$, can be calculated using Equation (10) as:

$$R_{CD} = \left(\frac{1}{4\pi} \sum_{n=1}^{N} \sum_{f > 30\ MHz}^{300\ GHz} \frac{P_{T,f}.G_{A,f}}{S_{inc,RL,f}} \right)^{1/2} \quad (10)$$

As 5G uses highly massive Multi Input Multi Output (mMIMO) systems that reduce interference and boost the cell capacity [31], more factors and variables were taken into account in several recent investigations of EMF exposure [19], [20], [32], [33], [34], [35], such as the system load, actually emitted power, duty cycle, and spatio temporal. Additionally, it was mentioned in [28] that EMF evaluation might be carried out for actual circumstances. In [35], [36], [37], their results found that the actual exposure level is quite lower compared to the theoretical exposure for 5G mMIMO. In this investigation, the research team continued the work related to the previous study [38], and added the power weight ρ_w as a reduction in the entire used power P_T which is used to calculate the power density [39], [40], [41], [42]. Thus, Equation. (10) changed to Equation. (11) which presents the compliance distances R_{CD}.

$$R_{CD} = \left(\frac{1}{4\pi} \sum_{n=1}^{N} \sum_{f > 30\ MHz}^{300\ GHz} \frac{\rho_{w,f}.P_{T,f}.G_{A,f}}{S_{inc,RL,f}} \right)^{1/2} \quad (11)$$

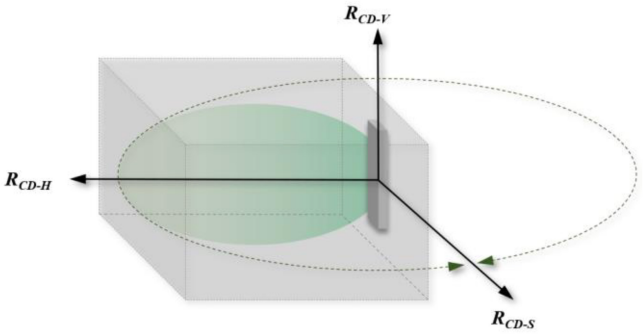

Illustration of the box-shape (horizontal, vertical, and side) that is appropriate for the CD boundaries of the sectorized site.

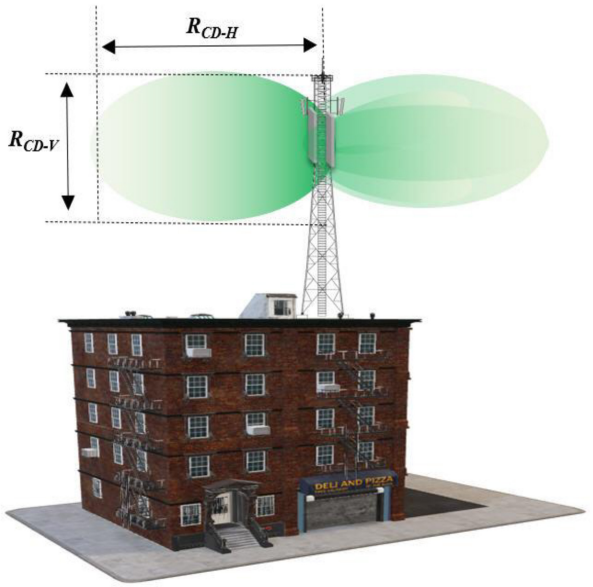

Illustration of the Horizontal R_{CD-H} and Vertical R_{CD-V} compliance distances for macro site installed on rooftop tower.

FIGURE 3. A.Illustration of the box-shape (horizontal, vertical, and side) that is appropriate for the CD boundaries of the sectorized site. B.Illustration of the Horizontal R_{CD-H} and Vertical R_{CD-V} compliance distances for macro site installed on rooftop tower.

In this study, the considered 5G technology uses a TDD high-grade mMIMO solution with dynamic beamforming. So, in Equation (11) the $P_{T,f}$ is multiplied by the power reduction factor $p_{w,f}$ which reflects the actual power of mMIMO with beamforming in the power density calculation, note that there are no changes applied for the algorithm and mechanism that control the beamforming performance, and only the 5G antenna body main direction is changed. Therefore, no changes in the whole envelope of all possible beams, and the test results described in Section VII-C show the coverage level (in term of SS-RSRP) of 5G remains the same before and after applying the solution.

The value of power reduction factor ρ_r for 5G TDD mMIMO depends on the TDD duty cycle and the spatial distribution, in this study the value of $\rho_r = 0.22$ is used for calculation in Equation (11) based on the work in [40], [41] who reported that actual power of TDD mMIMO varies between 7% and 22% of the maximum possible output power when maximum system load is considered, therefore the maximum value is considered as 0.22.

VI. TER AND CD SIMULATION FOR 3-SECTORS BS

In the three-sector model, the sector's directions are horizontally separated by 120 degrees, so in this study, the model uses 0/120/240 degrees for sectors 1/2/3. This section discusses the theoretical TER and CD figures calculated for different scenarios of BSs that use a three-sector and examines the de-concentration options by using different azimuths for antenna directions.

Table 3 lists a typical configuration for a three-sector site used for the TER and CD calculations. The BS is equipped with 6 technologies that transmit at the same time (GSM at 900 MHz, UMTS at 900 MHz, LTE at 800/1800/2100 MHz, and NR at 2600 MHz). In many countries, some operators run the 5G NR at higher frequencies such as 3.5GHz, or millimeter waves (mM) 28/39 GHz, but here the 5G NR is taken at 2.6 GHz because the calculations are validated in real-life sites operating with the frequencies and configurations listed in Table 3. Also, the 5G sites in this study were equipped with mMIMO 64T/64R radiating from Active Antenna Unit (AAU), which is a physical hardware device made up of an antenna and an integrated radio unit, most of technology providers designed the AAU as a small, workable alternative to employing a lot of antennas, such the 64 antennas needed to transmit the 64T/64R mMIMO. Here, the 5G AUU has 24.8 dBi gain and 65 degrees horizontal bandwidth (BW-H) for the envelope broadcast beam

It's crucial to highlight the following remarks about the used configuration in this study:

- Indirectly, both Horizontal BW and Vertical BW are considered in the CD calculations, because the value of the antenna gain $G_{A,f}$ in Equations (9) and (11) is taken from the antenna pattern according to the Gain at the measurement angle.
- The steering is not done for the beam, it's done for the antenna body, so the whole antenna pattern is redirected without changes in the BW itself. Therefore, the whole coverage for each layer was slightly rotated, but the coverage wasn't affected because the three sectors as one group provides continuous coverage in the area.
- In Section VI, Table 3 listed the used configuration in this study which is commonly deployed in life networks inside cities. The used antenna H-BW is between 60-65 degrees that typically used in three sector sites to provide continuous coverage.
- The proposed solution is mainly applicable inside cities and towns where each site provides continuous coverage surrounding the site location. However, it might give different results for remote areas and coverage along highways (roads) where narrow beamwidth antennas are used, this is an interesting topic that requires further studying and investigation.

TABLE 3. The configurations of 3-Sector BS site with 6 technologies.

Site Setting	2G 900	3G 900	4G 800	4G 1800	4G 2100	5G 2600
Freq. Band (MHz)	900	900	800	1800	2100	2600
Freq. BW (MHz)	4	4.2	10	10	20	60
Number of Tx	2T	1T	2T	2T	4T	64T
Number of Rx	2R	2R	2R	4R	4R	64R
Tx Power (Watt)	40	40	40	60	60	200
System Load	95%	95%	95%	95%	95%	95%
Ant. Gain (dBi)	16.6	16.6	16.2	16.5	17	24.8
Horizontal BW	60°	60°	65°	65°	65°	65°
Vertical BW	7.5°	7.5°	7.8°	6°	6°	6.5°
Ant. Tilt Angle	-6°	-6°	-6°	-6°	-6°	-6°
Ant. Height	35 m	35 m	35 m	35 m	35 m	35 m

Mathematical simulations are carried out to determine the TER and CD results for the proposed model using Equation (9) for the antenna's azimuths compared to the normal default azimuths where all antennas have the same direction. In this simulation, The TER and CD are calculated for two types of scenarios as follows:

- Scenario A: Applying the default azimuth, where all the antennas (of one sector) are directed in the same azimuth angle, this includes all technologies that transmit toward one direction. This design is commonly deployed in life networks where all technologies in one sector are connected to one multi-band antenna, or separate antennas but directed in one direction. For both, all transmitters radiate in the same sector direction as illustrated in Fig. 4.A.
- Scenarios B, C, D, E, F: Applying the proposed model by using different azimuths, the angle separation for each technology is calculated using Equation (9). In B, two antennas are used per sector, the first antenna transmits the 900/800/1800/2100 MHz, and the second antenna transmits the 2600 MHz. In C, three antennas are used per sector (1: G900/U900/L800, 2:

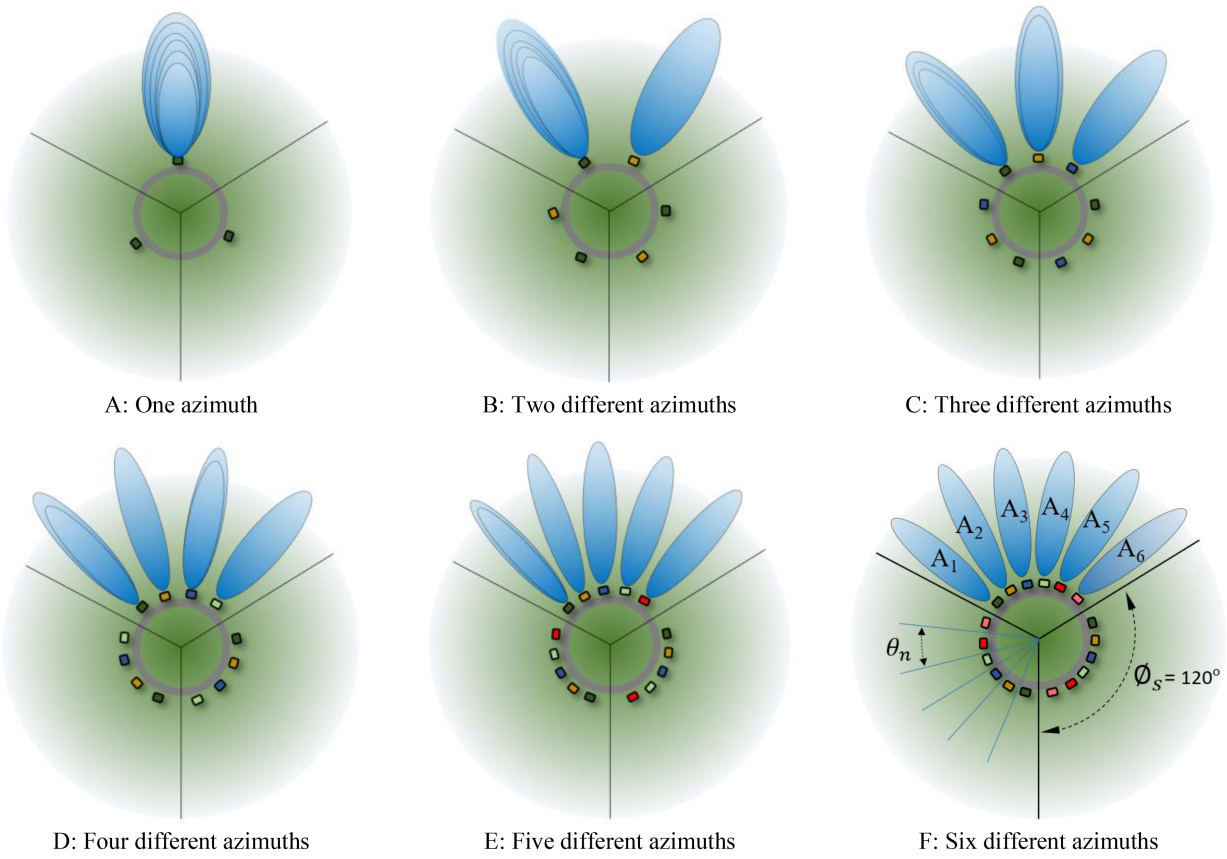

FIGURE 4. Illustration of using different numbers of antennas in one sector in the 3-sectors model.

L1800/L2100, 3: N2600). In D, four antennas are used (1: G900/U900, 2: L800, 3: L1800/L2100, 4: N2600). In E, five antennas are used (1: G900/U900, 2: L800, 3: L1800, 4: L2100, 5: N2600). In F, six antennas are used (1: G900, 2: U900, 3: L800, 4: L1800, 5: L2100, 6: N2600). Practically, the RF engineers design the antennas according to the site requirements and of course consider the company's strategy for deploying the technologies as most of the networks start with the classic system (2G, and 3G), then grow to advanced solutions including 4G and 5G.

in Scenarios B-F, the different technologies (different bands) transmit from different antennas, but all are placed at the same height on the tower, at 35m as listed in Table 3. Actually, installing the antennas at the same height is practically common use and routinely applied by MNOs due to simplicity for installation, accessibility for maintenance, and control of the traffic and coverage for interoperability between different technologies.

The simulation results are concluded in Table 4 listed the θ_n values for each technology (antenna) calculated for the corresponding scenario. Also, it shows the CD distances (in meters) reference to ICNIRP for the general public [43], [44], also it lists the reduction percent compared to the default setup using one direction for all technologies of scenario A. The results show that using 2 azimuths in scenario B gives less compliance distance by 23.3% compared to scenario A which has one direction. The 3 azimuths in scenario C gives 35.9% less CD, the 4 azimuths in scenario D gives 39.8% less CD, the 5 azimuths in scenario E gives 41.3% less CD, and the 6 azimuths in scenario F gives 43.4% less CD. Furthermore, Table 5 lists more detailed results of the horizontal and vertical compliance distances for the mentioned six scenarios references to both standards ICNIRP and FCC limits.

VII. IN SITU ASSESSMENT FOR TER DECONCENTRATION

A field experiment is done in a life network to examine the results of the proposed model by implementing the antenna's azimuths with angles calculated using Equation (9). To have an accurate result, the experiment is done for 4 Macro BS sites (one cluster) that service a residential populated district at Khubar city in the Kingdom of Saudi Arabia as shown in Fig. 5. The 4 sites belong to one public land mobile network operator (PLMN), all sites have the same configuration of three-sector, and each is equipped with 6 systems that transit as co-located in a multi-technology site.

The 4 sites use 0/120/240 degrees model for the sector's azimuths, where the 0 degree starts from the north geographical direction and increases clockwise. All the sites

TABLE 4. The configurations of 3-Sector BS site, and equipped with 6 technologies.

Antenna's Azimuths	Sector Configuration (Multi-Technologies)	Separation Angles Θ_n (degrees)						CD (m)	CD Reduction (%)
		G9	U9	L8	L18	L21	N26		
1 Azimuth	(G9/U9/L8/L18/L21/N26)	120.0°						15.58	0.00%
2 Azimuths	(G9/U9/L8/L18/L21), (N26)	70.3°					49.7°	12.63	-23.3%
3 Azimuths	(G9/U9/L8), (L18/L21), (N26)	47.9°			22.4°		49.7°	11.45	-35.9%
4 Azimuths	(G9/U9), (L8), (L18/L21), (N26)	30.4°		17.5°	22.4°		49.7°	11.13	-39.8%
5 Azimuths	(G9/U9), (L8), (L18), (L21), (N26)	30.4°		17.5°	11.2°	11.3°	49.7°	11.02	-41.3%
6 Azimuths	(G9), (U9), (L8), (L18), (L21), (N26)	15.2°	15.2°	17.5°	11.2°	11.3°	49.7°	10.85	-43.4%

TABLE 5. The horizontal and vertical compliance distances for the general public and occupational workers reference to ICNIP and FCC reference limits.

Antenna's Azimuths	Sector Configuration (Multi-Technologies)	ICNIRP GP (m)		ICNIRP OW (m)		FCC GP (m)		FCC OW (m)	
		CD_H	CD_V	CD_H	CD_V	CD_H	CD_V	CD_H	CD_V
1 Azimuth	(G9/U9/L8/L18/L21/N26)	15.58	2.51	6.97	1.12	14.70	2.29	6.57	1.02
2 Azimuths	(G9/U9/L8/L18/L21), (N26)	12.63	1.92	5.34	0.86	11.27	1.76	5.04	0.79
3 Azimuths	(G9/U9/L8), (L18/L21), (N26)	11.45	1.60	4.46	0.72	9.41	1.47	4.21	0.66
4 Azimuths	(G9/U9), (L8), (L18/L21), (N26)	11.13	1.51	4.19	0.67	8.84	1.38	3.95	0.62
5 Azimuths	(G9/U9), (L8), (L18), (L21), (N26)	11.02	1.47	4.09	0.66	8.63	1.34	3.86	0.60
6 Azimuths	(G9), (U9), (L8), (L18), (L21), (N26)	10.85	1.42	3.94	0.63	8.31	1.30	3.72	0.58

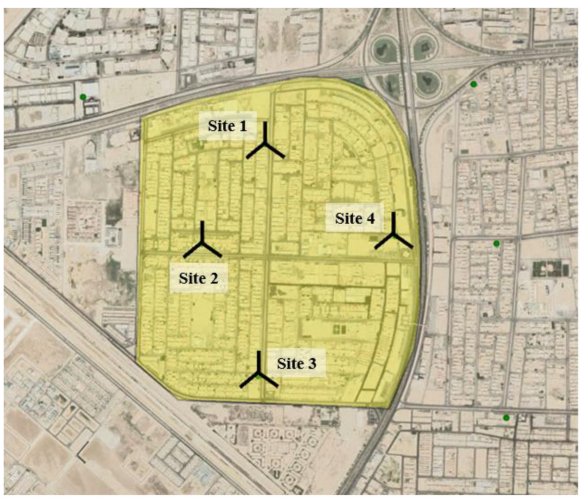

FIGURE 5. Google Earth map for the 4 sites where the field experiment is done.

were deployed with scenario B using two antennas, one for G9/U9/L8/L18/L21, and the second antenna for N26. Initially, all antennas were directed toward the same azimuth and were transmitted in the same direction. Then, the 2^{nd} antennas of all sectors are redirected (rotated) to new directions with azimuths 60/180/300 degrees which gives 60 degrees as the horizontal separation angle between each two antennas in each sector.

Two types of data are collected to assess the total exposure before and after applying the antenna azimuth changes, and also to evaluate the effects (impact) on the coverage signal level and capacity, as follows:

- Power density field measurement (radiation meter).
- TER from Geo-location data (system records).
- Signal level field measurements (drive test).
- Network's OSS KPIs data (system records)

A. POWER DENSITY FIELD MEASUREMENT

Field measurements are conducted to measure the power density from two points in Site 1 (P1 and P2) as shown in Fig. 6, and also from two points in Site 2 (P3 and P4) as shown in Fig. 7. The locations P1 and P3 are intentionally selected facing the initial direction of the antennas at 0/120/240 degrees, and locations P2 and P4 are selected facing 60/180/300 degrees.

The SRM-3006 Narda [45] radio selective radiation meter is used for the measurements, this tool supports a frequency range from 9.0 kHz to 6.0 GHz, and has a three-axis isotropic antenna (E-field). Fig. 8 shows the site and the meter position during the field test at the selected site, and the meter was positioned facing the primary beam direction of the antenna at a height of 2 meters on a tripod.

The SRM-3006 was configured to scan the downlink (DL) frequency ranges, the team collected approximately 7,200 measurement samples for each system technology at each point with a scan rate of 0.67 sample/second. To have an accurate evaluation, all measurements are conducted during the same time during the highest hours of traffic (from 07:00 to 10:00 pm). For each point, the measurements are done

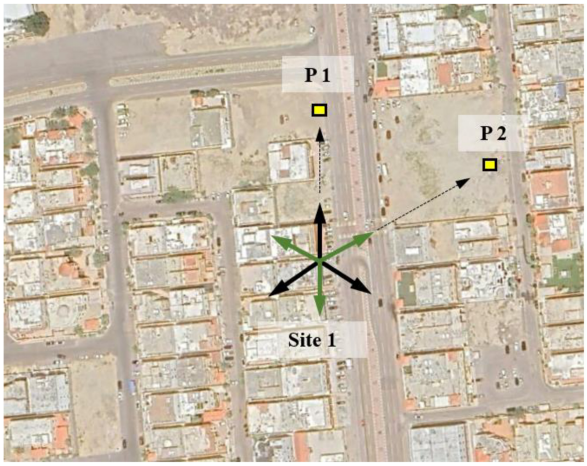

FIGURE 6. Site 1, locations of P1 and P2 measurements.

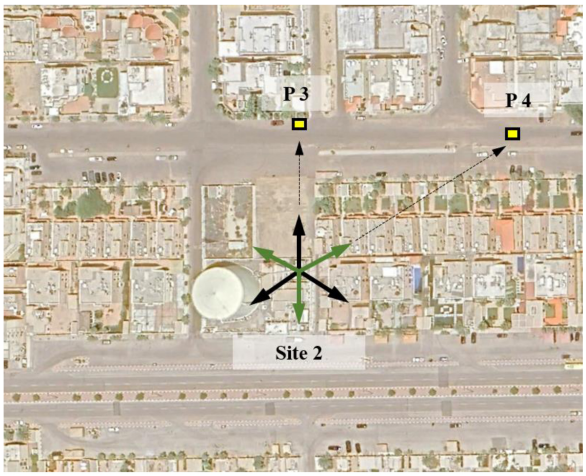

FIGURE 7. Site 2, locations of P3 and P3 measurements.

twice, before the antenna's azimuth changes (Pre), and after the azimuth change (Post).

Table 6 lists the results of the measured power density and TER at each point (for both Pre-and-Post measurements). The results from site 1 show that TER decreased at point 1 by −5.41% while it increased at P2 by 5.95% with reference to the ICNIRP limit. Also, the results for site 2 show that TER decreased at point 1 by −5.52% while it increased at P2 by +5.05% with reference to the ICNIRP limit. Furthermore, Table 6 listed the TER increase/decrease for sites 1 and 2 in reference to FCC limits.

To control the measurement and avoid significant errors due to scanning unwanted power density from other radiators, the following method is applied:

- The SRM-3006 was configured and locked to scan the frequency ranges of the technologies of the test sites.
- The SRM-3006 was configured to scan only the Downlink (DL) power densities, because Uplink (UL) radiation cannot be controlled (before and after applying the solution) which comes from user equipment handsets (UEs).

FIGURE 8. The measurement location where the radiation meter is placed in front of the antennas for the multi-technology site.

B. TER EVALUATION FROM GEO-LOCATION DATA

The TER is evaluated for the whole cluster before and after the antenna changes (Pre-and-Post) using the geo-location data recorded in the OSS system. The network OSS archives the daily (and hourly) statistics and information about network traffic and performance, this includes counters and key performance indicators. It also includes geo-location data that contains the information associated with handset devices connected to the network such as the radio conditions (received signal level, channel quality, etc..) with the associated coordinates.

The received levels of all technologies from all devices in the cluster (within the polygon of the test area) are recorded before and after the azimuth changes, and it's used to calculate the TER [42]. The geo-location system gives the data as average for pixels of 50x50 meters each, the area under this test consists of 954 pixels within the cluster polygon of 2.3 Km^2.

The geolocation data is collected and calculated for two weeks duration, one week before and one week after the antenna azimuth change. Fig. 9 summarizes the results which show the average Pre TER is $23.4x10^{-6}$, and it decreased to $18.91x0^{-6}$ after antenna azimuth is changed, this reduction is an improvement of −19.23% in average TER.

TABLE 6. The measured power density and TER before and after the antenna's Azimuth changes.

Measurement	Site	Site 1: PD (mW/m^2)				Site 2: PD (mW/m^2)			
	Location	P1		P2		P3		P4	
		Pre	Post	Pre	Post	Pre	Post	Pre	Post
Power Density (mW/m^2)	G900	0.26	0.26	0.21	0.21	0.23	0.23	0.21	0.21
	U900	0.91	0.91	0.80	0.80	0.15	0.15	0.13	0.13
	L800	0.43	0.43	0.33	0.33	0.49	0.49	0.39	0.39
	L1800	1.12	1.12	1.02	1.02	1.15	1.15	1.05	1.05
	L2100	2.04	2.04	2.00	2.00	2.02	2.02	1.82	1.82
	N2600	5.85	5.15	4.86	5.52	6.39	5.74	5.59	6.11
ICNIRP GP	TER	0.0013	0.0012	0.0011	0.0012	0.0012	0.0011	0.0010	0.0011
	TER (%)		-5.41%		5.95%		-5.52%		5.09%
FCC GP	TER	0.0012	0.0011	0.0010	0.0011	0.0017	0.0016	0.0015	0.0016
	TER (%)		-5.89%		6.47%		-6.23%		5.71%
ICNIRP OW	TER	0.0003	0.0002	0.0002	0.0002	0.0002	0.0002	0.0002	0.0002
	TER (%)		-5.41%		5.95%		-5.52%		5.09%
FCC OW	TER	0.0002	0.0002	0.0002	0.0002	0.0002	0.0002	0.0002	0.0002
	TER (%)		-5.89%		6.47%		-5.84%		5.37%

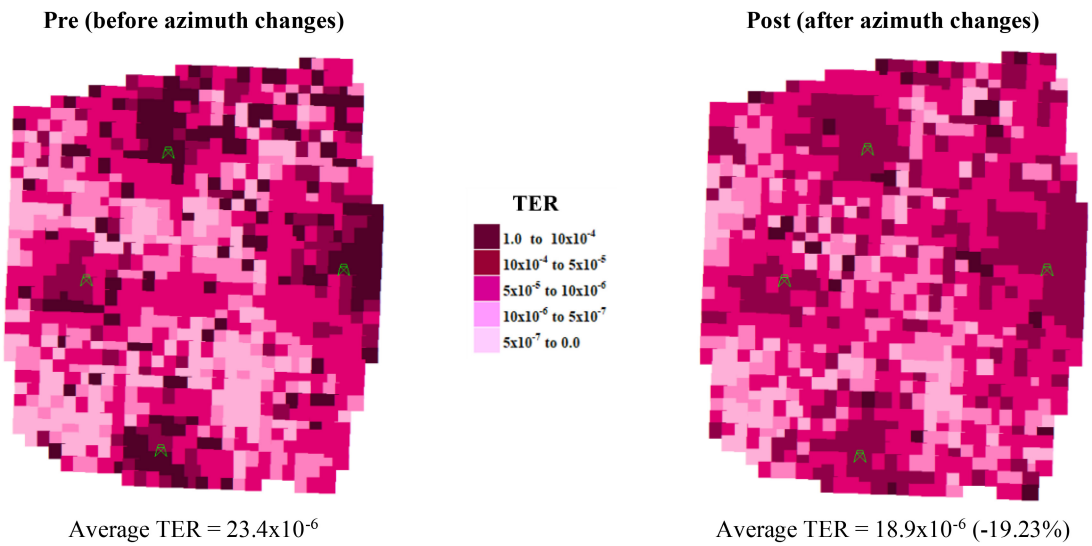

FIGURE 9. The Pre and Post average TER from the geo-location records.

Also, the TER distribution is evaluated and the results show that the higher range of TER (1.0 to $10x10^{-4}$) was counted for 17.0% on total pixels before the antenna changes, and it decreased to 2.7% after antenna azimuth was changed as listed in Table 7. As a consequence, results, the lower range of TER ($5x10^{-7}$ to 0.0) is increased from 16.7% to 10.2%. These results state that the total exposure is deconcentrated when separate directions are used for antennas azimuths.

TABLE 7. The TER distribution (pre and post) for the whole cluster.

TER	Pre		Post	
	Pixel Count	Pre %	Pixel Count	Post %
1.0 to $10x10^{-4}$	162	17.0%	26	2.7%
$10x10^{-4}$ to $5x10^{-5}$	98	10.3%	269	28.2%
$5x10^{-5}$ to $10x10^{-6}$	368	38.6%	399	41.8%
$10x10^{-6}$ to $5x10^{-7}$	167	17.5%	163	17.1%
$5x10^{-7}$ to 0.0	159	16.7%	97	10.2%
Total Pixel	**954**		**954**	

C. SIGNAL LEVEL FIELD MEASUREMENT

Drive test field measurements were conducted to evaluate the effect of azimuth rotation on the network received signal levels from all technologies. The team used Test of Mobile System (TEMS) Investigation v20 [46] which was installed on a laptop PC and connected to GPS and three mobile user equipment (UE), as seen in Fig. 10. The UEs were mounted inside a vehicle in front of the dashboard at a

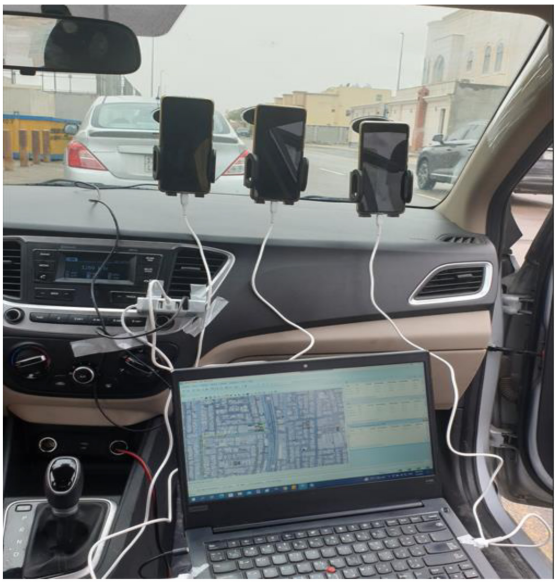

FIGURE 10. The tool setup for field drive test measurements.

TABLE 8. The pre and post Rx levels from drive test measurements.

Measurement Layer		G 900 BCCH	U 900 RSCP	L 800 RSRP	L 1800 RSRP	L 2100 RSRP	N 2600 SS-RSRP
Average Rx Level (dBm)	Pre	-68.9	-72.1	-77.6	-82.9	-83.3	-79.2
	Post	-69.3	-71.3	-77.0	-82.0	-82.6	-79.6
	Delta (dB)	0.4	-0.8	-0.6	-0.9	-0.7	0.4

height of 1.3 to 1.5 meters from the ground, and each UE was locked to measure single technology Rx signal level. The measured samples were taken every 0.5 seconds for each UE, with over 3,290 measurement samples for each technology. The measurements are stored in log files together with the relevant time and GPS coordinates. The collected measurements include the Rx signal level in dBm of the Broadcast Common Control Channel (BCCH) for 2G, the Received Signal Code Power (RSCP) for 3G, the Reference Signal Received Power (RSRP) for 4G, and the Secondary Synchronization Reference Signal Received Power (SS-RSRP) for 5G.

The drive test log files are imported and post-processed using MapInfo Pro software [47], and the Rx levels for each technology are evaluated for pre-and-post measurements. Table 8 summarizes the results that show the average coverage level in dBm and the delta of Pre vs Post, it indicates that there is no major drawback in signal level in the whole cluster for all technologies.

For example, in Fig. 11 and 12, the Rx levels are plotted in the cluster map to display the details of the coverage levels and distribution for L800 and N2600 technologies. The results show the RSRP for L800 almost remains at the same average levels with −77.6 dBm at Pre and −77.0 dBm at Post with −0.6 dB delta, and have the same RSRP accumulated distribution among the cluster area. Also, the same results are obtained for N2600, the SS-RSRP almost remains at the same levels with −79.2 dBm at Pre and −79.6 dBm at Post with 0.4 dB delta. The minor differences in the measurements Pre vs Post are due to the rotation of the antenna directions where some locations have received higher signal levels and some have received lower levels compared to before applying the model depending on the antenna's main beam directions, mainly this due to the constructions in the area (the buildings and houses) as it remains in the same places while the antenna's directions have been changed which affect the signal propagation.

D. OSS PERFORMANCE RECORDS

Operation support system for mobile networks often uses system row counters and statistics typically refer to a variety of metrics and data records that aid in network performance management and monitoring [37]. In this work, some of OSS key performance indicators (KPIs) are employed to evaluate the behavior of the cluster under this study before and after applying the antenna azimuth changes which were implemented on the 09^{th} of January 2024. The daily data were recorded for a continuous six weeks, three weeks pre, and three weeks post to the date of the change.

Fig. 13 shows the total daily carried traffic by the 5G N2600 for the whole cluster (4 sites), and also the system load percentage recorded based on the physical resource block (PRB) utilization. The traffic trend shows no significant change after the implementation date where the average traffic was 1.16 TB and became 1.18 TB, and the PRB utilization was 14.4% and became 14.5% with 0.7% increment.

Also, for N2600, Fig. 14 shows the daily total number of active connected users (simultaneous connection) and the user's throughput, the trend shows a very slight increase in connected users from an average of 295 to 305 users per day. And, there was almost no significant change in the user's throughput which was 78.7 Mbps and became 78.3 Mbps with −0.6% reduction.

Another two important metric performance indicators are collected, the admission call setup success rate (CSSR) and the HO success rate (HOSR), and for both the daily trend remains within the same average values as shown in Fig. 15 where CSSR was 99.8% during Pre and Post, and the HOSS was 99.0% with slightly decreased to 98.9% with −0.1% reduction.

Although the daily KIPs results reflect the overall performance, it's important to look into the Busy Hour (BH) which represents around 14.8% of the total daily traffic carried in the test area. Overall, the BH performance OSS KPIs show no impact after applying the proposed model. As an example, for the 5G technology which is the most important layer that has the highest contribution to the total exposure ratio, Fig. 16 shows the BH carried traffic by the 5G N2600 for the whole cluster (4 sites), and also the system utilization load percentage, the trend shows no significant change after the implementation date where the

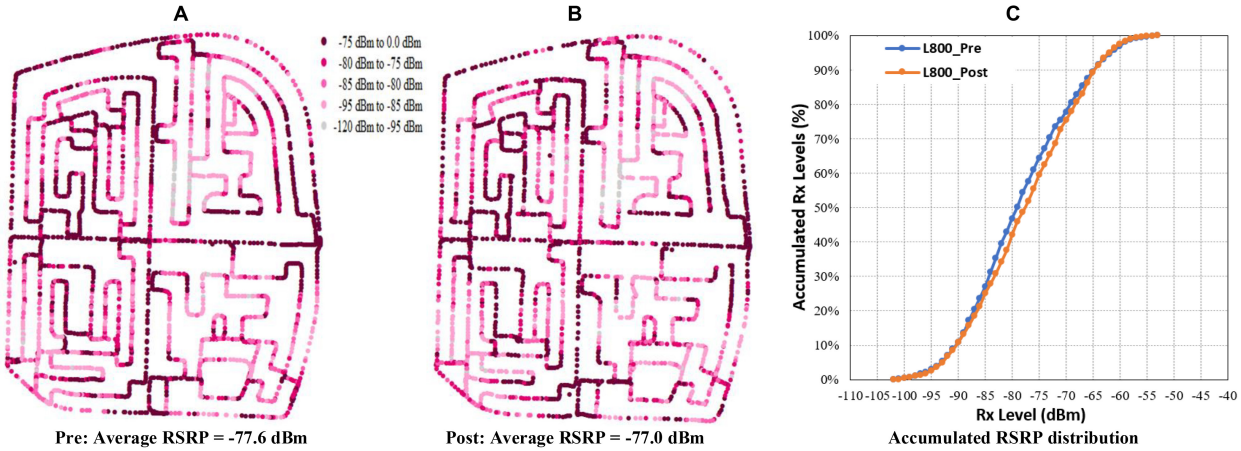

FIGURE 11. The 4G L800 MHz (A) Pre RSRP level (B) Post RSRP level (C) Accumulated RSRP.

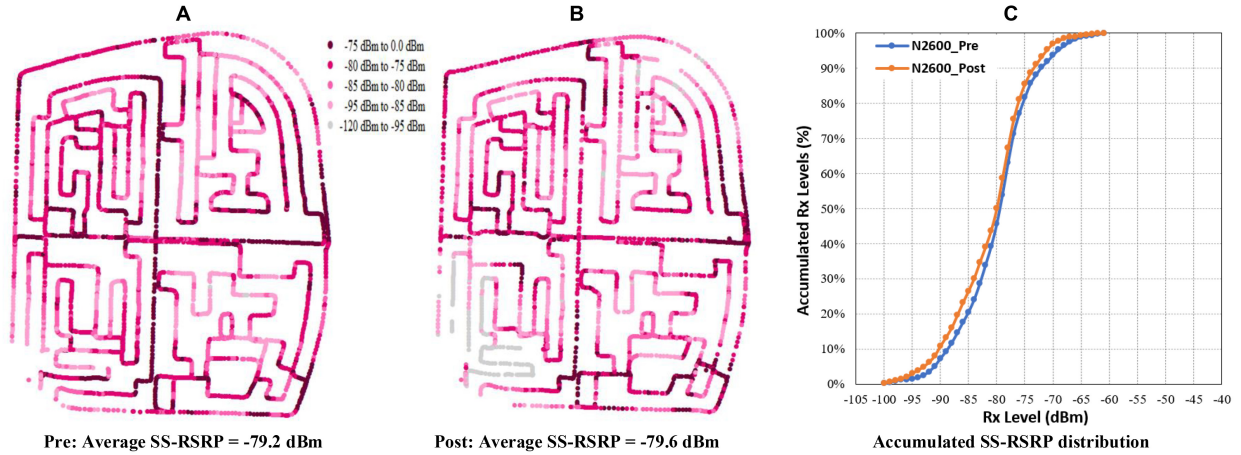

FIGURE 12. The 5G N2600 MHz (A) Pre SS-RSRP level (B) Post SS-RSRP level (C) Accumulated SS-RSRP.

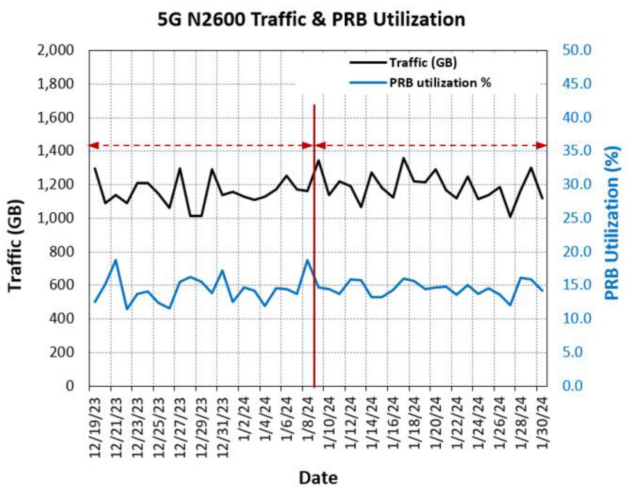

FIGURE 13. The daily total carried traffic and the radio physical resources utilization of the 5G N2600 for the whole cluster.

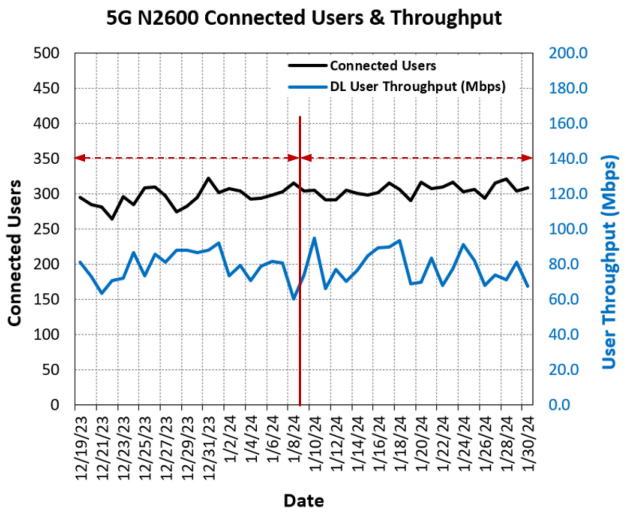

FIGURE 14. The daily total active connected users and user's throughput of the 5G N2600 for the whole cluster.

BH traffic was 173.1 GB and became 173.5 GB with 0.2% increase, and the PRB utilization was 26.0% and remain with same figure 26.0%. Also, for N2600, Fig. 17 shows the BH number of actively simultaneous connected users and the user's throughput, the trend shows a very slight increase in connected users from 267.1 to 267.5 users (0.2% increase). And, almost there was no change in the user's throughput

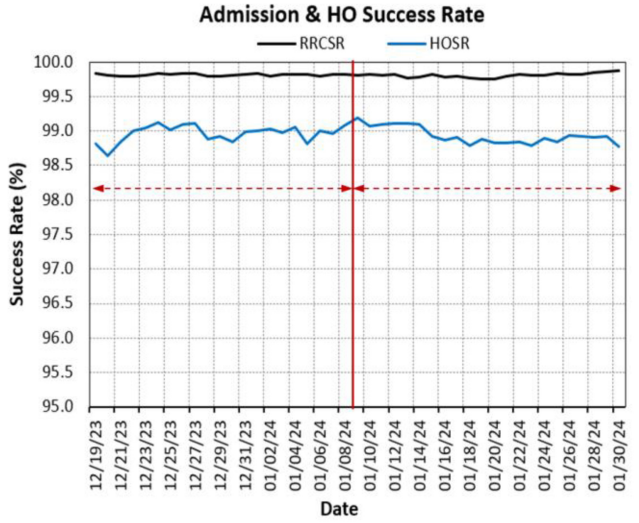

FIGURE 15. The daily call setup and handover success rates of the 5G N2600 for the whole cluster.

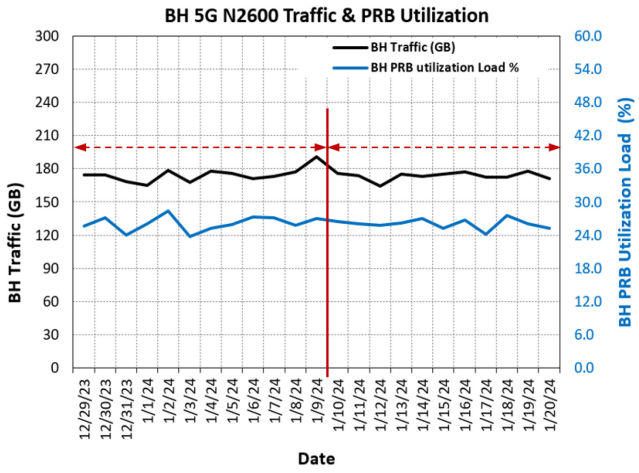

FIGURE 16. The BH carried traffic and the radio physical resources utilization of the 5G N2600 for the whole cluster.

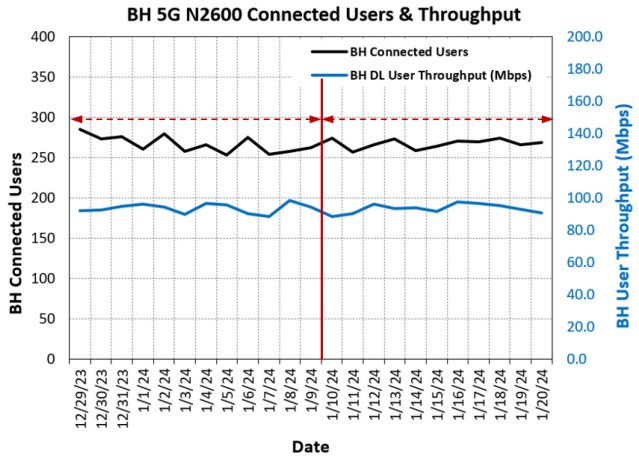

FIGURE 17. The BH active connected users and user's throughput of the 5G N2600 for the whole cluster.

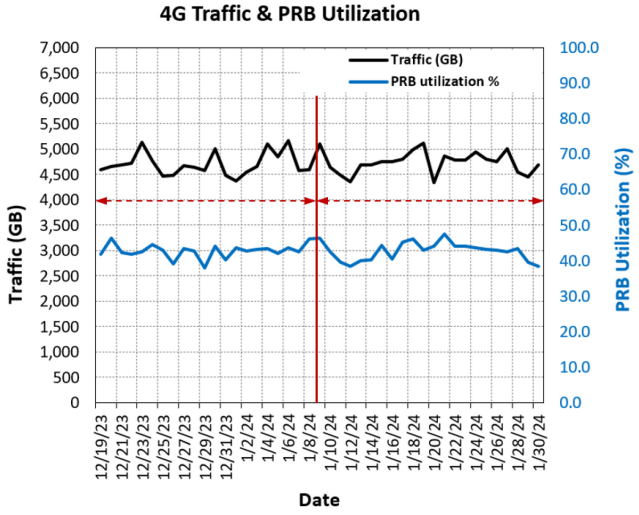

FIGURE 18. The daily total carried traffic and the radio physical resources utilization of the 4G LTE for the whole cluster.

which was 93.5 Mbps and became 93.4 Mbps with a very slight reduction −0.1%.

Very similar behavior was observed for the 4G technologies from the OSS records which are collected for all LTE cells (including L800, L1800, and L2100) and combined to generate LTE reports for the whole cluster. Fig. 17 shows the total daily carried traffic by the 4 LTE sites and their PRB utilization. The traffic trend displays no significant effect after the implementation date where the average traffic was 4.71 TB and became 4.72 TB with 0.5% increment, and the PRB utilization was 42.7% and became 42.5% with −0.4% reduction.

Likewise, Fig. 19 shows the active connected users were 999 and became 1,008 users with a 0.9% increment. The user's throughput was 20.4 Mbps and became 20.3 Mbps with a −0.4% reduction. Also, Fig. 20 displays that both CSSR and HOSR remain with the same percentages at 99.9% with no changes before and after the implementation date.

Although the 2G and 3G technologies are on the way to being switched off, it's still carrying some traffic in this cluster and it's included in the implemented antenna azimuths in this test. Similar to LTE and NR, the OSS records show no major change in 2G and 3G performance.

Fig. 21 shows the total daily carried traffic by all 3G sites with CSSR and HOSR, the traffic trend displays no significant effect after the implementation date where the average traffic was 276 GB and became 277 GB with a 0.6% increment, and both CSSR and HOSR remains with the same percentages at 99.9%.

Finally, for all 2G sites, Fig. 22 shows the CSSR and HSSR trends with no major changes, and both remain with the same percentages at 99.9%.

VIII. APPLICATIONS OF THE PROPOSED MODEL

Reducing the TRE is the goal of the suggested method, and doing so will inevitably shorten compliance distances. On

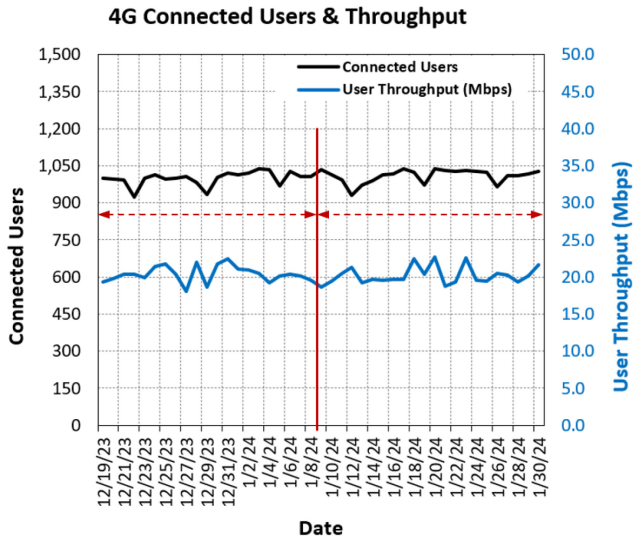

FIGURE 19. The daily total active connected users and user's throughput of the 4G LTE for the whole cluster.

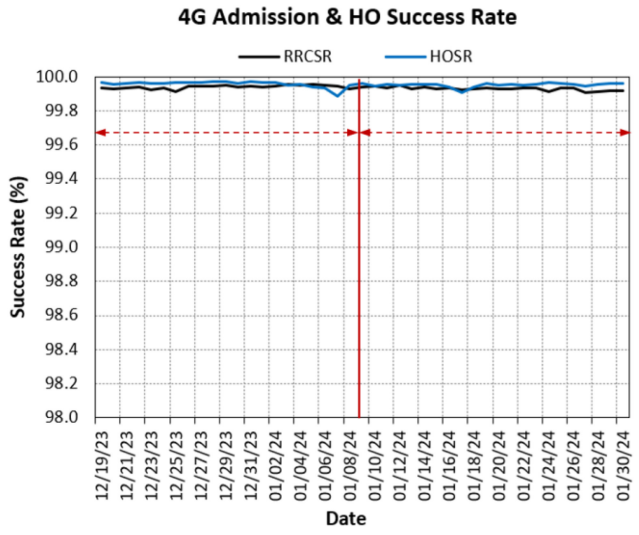

FIGURE 20. The daily call setup success rate and handover success rate of the 4G LTE for the whole cluster.

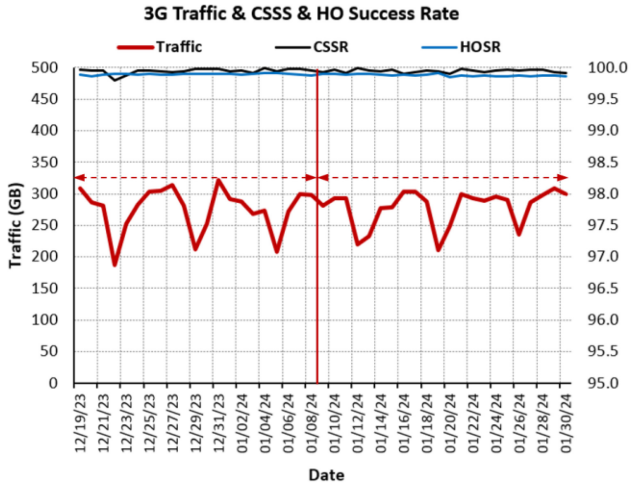

FIGURE 21. The daily traffic, call setup success rate, and handover success rate of the 3G UMTS for the whole cluster.

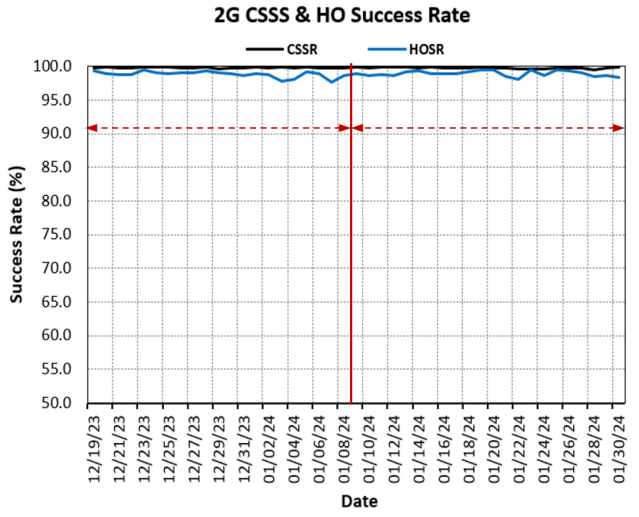

FIGURE 22. The call setup success rate and handover success rate of the 2G GSM for the whole cluster.

the other hand, neither the site performance nor the site coverage levels are impacted by the suggested approach.

Nearly all national regulators require that the compliance borders be exclusive, inaccessible areas for the general public and shall be marked with warning signs or other obstacles to keep people out. To implement the compliance requirement, it is necessary to determine the compliance distances. The easier it is for mobile operators to meet the standards, the lower the compliance limits. The authors see these requirements can be assessed in the design phase before implementation, and small adjustments to the antenna orientations can be made using the proposed model to shorten the compliance distances for the necessary cases, particularly for wall-mounted and rooftop sites where the antennas usually will be placed in close proximity to accessible areas.

Also, the mobile operators continue expanding their networks by adding and deploying new technologies such as the 5G NR into the existing on-air sites following the current sector's direction, this approach increases the total exposure ratio and consequently extends the compliance boundaries. For some sites, extending the compliance boundaries to bigger ranges might reach accessible areas specifically for some rooftop and wall-mounted sites. in these kinds of situations, the authors believe that the proposed solution is advantageous and can assist in reducing the compliance distances without affecting network performance or coverage.

IX. CONCLUSION

There is growing worry over the possibility of increasing exposure to electromagnetic field radiation due to the enormous deployment of mobile base stations. A design model to de-concentrate the overall exposure ratio from sectorized

antennas of the multi-technology base station was presented in this study. The model uses the weighted antenna's azimuth to spread the total exposure by horizontally separating the installed antennas in the same sector. A set of simulations is carried out to calculate the reduction in total exposure for widely commonly used antenna deployment setups in multi-technology mobile networks. For three-sectors BS operating with six technologies, the simulation results show the compliance distance is reduced by −23% when using two antennas (two different azimuths) compared to using one azimuth, reduced by −35.9% using 3 azimuths, −39.8% using 4 azimuths, −41.3% using 5 azimuths, and by −43.4% when using 6 azimuths. A field test is done in a life network serving in a geographical cluster that consists of 4 sites, the results show that the TER is reduced by −19.23% after the antennas azimuths are changed with separation angles calculated using the proposed model. Further, the OSS system performance records and counters were analyzed to evaluate the impact of the model on the network coverage and capacity. Overall, the system records show no significant impacts were registered on network coverage level and capacity performance for all transmitting technologies of the sites involved in the test . The proposed solution is beneficial and can help mobile operators minimize the compliance boundaries without impacting the network coverage and performance, especially for rooftop and wall-mounted sites where the antennas are installed in close areas accessible to the general public.

REFERENCES

[1] A. Bajpai and A. Balodi, "Role of 6G networks: Use cases and research directions," in *Proc. IEEE Bangalore Humanitarian Technol. Conf. (B-HTC)*, 2020, pp. 1–5, doi: 10.1109/B-HTC50970.2020.9298017.

[2] M. Z. Chowdhury, M. Shahjalal, S. Ahmed, and Y. M. Jang, "6G wireless communication systems: Applications, requirements, technologies, challenges, and research directions," *IEEE Open J. Commun. Soc.*, vol. 1, pp. 957–975, 2020, doi: 10.1109/OJCOMS.2020.3010270.

[3] W. J. Koh and S. M. Moochhala, "Non-ionizing EMF hazard in the 21st century," in *Proc. IEEE Int. Asia–Pac. Symp. Electromag. Compat. (EMC/APEMC)*, 2018, pp. 518–522, doi: 10.1109/ISEMC.2018.8393832.

[4] A. B. Sharma, O. S. Lamba, A. Sharma, and M. Sanadhya, "Investigation to measure risk free exposure from mobile base station antennas in residential area," in *Proc. 2nd Int. Conf. Micro-Electron. Telecommun. Eng. (ICMETE)*, 2018, pp. 64–70, doi: 10.1109/ICMETE.2018.00026.

[5] W. El-Beaino, A. M. El-Hajj, and Z. Dawy, "On Radio network planning for next generation 5G networks: A case study," in *Proc. Int. Conf. Commun., Signal Process., Appl. (ICCSPA)*, 2015, pp. 1–6, doi: 10.1109/ICCSPA.2015.7081315.

[6] C. Blackman and S. Forge, "5G deployment—State of play in Europe, USA and Asia," Dept. Policy Econ. Sci. Qual. Life Policies, Eur. Parliament, Brussels, Belgium, Rep. PE 631.060, Apr. 2019.

[7] L. Chiaraviglio, A. Elzanaty, and M.-S. Alouini, "Health risks associated with 5G exposure: A view from the communications engineering perspective," *IEEE Open J. Commun. Soc.*, vol. 2, pp. 2131–2179, 2021, doi: 10.1109/OJCOMS.2021.3106052.

[8] V. Markovic, "5G EMF exposure: Overview of recent research and safety standard updates," in *Proc. 15th Int. Conf. Adv. Technol., Syst. Services Telecommun. (TELSIKS)*, 2021, pp. 359–365, doi: 10.1109/TELSIKS52058.2021.9606262.

[9] M. Celaya-Echarri, L. Azpilicueta, J. Karpowicz, V. Ramos, P. Lopez-Iturri, and F. Falcone, "From 2G to 5G spatial modeling of personal RF-EMF exposure within urban public trams," *IEEE Access*, vol. 8, pp. 100930–100947, 2020, doi: 10.1109/ACCESS.2020.2997254.

[10] L. Chiaraviglio et al., "Planning 5G networks under EMF constraints: State of the art and vision," *IEEE Access*, vol. 6, pp. 51021–51037, 2018, doi: 10.1109/ACCESS.2018.2868347.

[11] L. Chiaraviglio, C. Di Paolo, and N. Blefari-Melazzi, "5G network planning under service and EMF constraints: Formulation and solutions," *IEEE Trans. Mobile Comput.*, vol. 21, no. 9, pp. 3053–3070, Sep. 2022, doi: 10.1109/TMC.2021.3054482.

[12] *Evaluating Compliance with FCC Guidelines for Human Exposure to Radiofrequency Electromagnetic Fields*, Federal Commun. Comm. Office Eng. Technol., Washington, DC, USA, 1997.

[13] Z. Sienkiewicz, "Guidelines for limiting exposure to electromagnetic fields (100 kHz to 300 GHz)," *Health Phys.*, vol. 118, no. 5, pp. 483–524, 2020.

[14] J. Herbertz, "Guidelines for limiting exposure to time-varying electric, magnetic, and eletromagnetic fields (up to 300 GHz). International commission on non-ionizing radiation protection," *Health Phys.*, vol. 74, no. 4, pp. 494–522, 1998.

[15] M. S. Elbasheir, R. A. Saeed, A. A. Z. Ibrahim, S. Edam, F. Hashim, and S. M. E. Fadul, "A review of EMF radiation for 5G mobile communication systems," in *Proc. IEEE Asia-Pac. Conf. Appl. Electromag. (APACE)*, 2021, pp. 1–6, doi: 10.1109/APACE53143.2021.9760689.

[16] M. S. Elbasheir, R. A. Saeed, and S. Edam, "5G base station deployment review for RF radiation," in *Proc. Int. Symp. Netw., Comput., Commun. (ISNCC)*, 2021, pp. 1–5, doi: 10.1109/ISNCC52172.2021.9615689.

[17] "Public policy." GSMA. 2019. [Online]. Available: https://www.gsma.com/publicpolicy/emf-and-health/emf-policy

[18] *Determination of RF Field Strength and SAR in the Vicinity of Radio Communication Base Stations for the Purpose of Evaluating Human Exposure*, IEC Standard IEC 62232:2022, Oct. 2022.

[19] B. Thors et al., "On the estimation of SAR and compliance distance related to RF exposure from mobile communication base station antennas," *IEEE Trans. Electromag. Compat.*, vol. 50, no. 4, pp. 837–848, Nov. 2008, doi: 10.1109/TEMC.2008.2004605.

[20] A. Jain and P. Tupe-Waghmare, "Radiation measurements at repeated intervals for various locations of SIU campus and calculation of compliance distance from cell tower," in *Proc. Int. Conf. Autom. Control Dyn. Optim. Techn. (ICACDOT)*, 2016, pp. 804–808, doi: 10.1109/ICACDOT.2016.7877698.

[21] M. Velghe, S. Aerts, L. Martens, W. Joseph, and A. Thielens, "Protocol for personal RF-EMF exposure measurement studies in 5th generation telecommunication networks," *Environ. Health*, vol. 20, no. 1, pp. 1–10, 2021.

[22] R. Werner, P. Knipe, and S. Iskra, "A comparison between measured and computed assessments of the RF exposure compliance boundary of an in-situ radio base station massive MIMO antenna," *IEEE Access*, vol. 7, pp. 170682–170689, 2019, doi: 10.1109/ACCESS.2019.2955715.

[23] D. Pinchera, M. Migliore, and F. Schettino, "Compliance boundaries of 5G massive MIMO radio base stations: A statistical approach," *IEEE Access*, vol. 8, pp. 182787–182800, 2020, doi: 10.1109/ACCESS.2020.3028471.

[24] A. Thielens, G. Vermeeren, D. Kurup, W. Joseph, and L. Martens, "Compliance boundaries for LTE base station antennas at 2600 MHz," in *Proc. 6th Eur. Conf. Antennas Propag. (EUCAP)*, Prague, Czech Republic, 2012, pp. 889–892, doi: 10.1109/EuCAP.2012.6205926.

[25] F. Héliot, T. H. Loh, D. Cheadle, Y. Gui, and M. Dieudonne, "An empirical study of the stochastic nature of electromagnetic field exposure in massive MIMO systems," *IEEE Access*, vol. 10, pp. 63100–63112, 2022, doi: 10.1109/ACCESS.2022.3182236.

[26] R. Joyce, D. Morris, S. Brown, D. Vyas, and L. Zhang, "Higher order horizontal sectorization gains for 6, 9, 12 and 15 sectored cell sites in a 3GPP/HSPA+ network," *IEEE Trans. Veh. Technol.*, vol. 65, no. 5, pp. 3440–3449, May 2016, doi: 10.1109/TVT.2015.2446945.

[27] C. Weng, H. Wang, K. Li, and M. N. S. Swamy, "Azimuth estimation for sectorized base station with improved soft-margin classification," *IEEE Access*, vol. 8, pp. 96649–96660, 2020.
[28] E. Degirmenci, B. Thors, and C. Törnevik, "Assessment of compliance with RF EMF exposure limits: Approximate methods for radio base station products utilizing array antennas with beam-forming capabilities," *IEEE Trans. Electromag. Compat.*, vol. 58, no. 4, pp. 1110–1117, Aug. 2016.
[29] T. Kopacz and D. Heberling, "Impact of the elevation scanning angle on the vertical compliance distance of 5G massive MIMO antennas," in *Proc. 13th Eur. Conf. Antennas Propag. (EuCAP)*, 2019, pp. 1–5.
[30] S. Liu, T. Onishi, M. Taki, and S. Watanabe, "Radio frequency electromagnetic field exposure compliance assessments of smart surfaces: Two approximate approaches," *IEEE Trans. Electromag. Compat.*, vol. 64, no. 4, pp. 963–974, Aug. 2022.
[31] K. Narongrit, P. Uthansakul, and M. Uthansakul, "Performance analysis of MB-MIMO under 120 degree sector consideration for 5G communications," in *Proc. 20th Asia-Pac. Conf. Commun. (APCC)*, 2014, pp. 463–467.
[32] H. Tataria, K. Haneda, A. F. Molisch, M. Shafi, and F. Tufvesson, "Standardization of propagation models for terrestrial cellular systems: A historical perspective," *Int. J. Wireless Inf. Netw.*, vol. 28, pp. 20–44, 2021. [Online]. Available: https://doi.org/10.1007/s10776-020-00500-9
[33] B. Thors, D. Colombi, Z. Ying, T. Bolin, and C. Törnevik, "Exposure to RF EMF from array antennas in 5G mobile communication equipment," *IEEE Access*, vol. 4, pp. 7469–7478, 2016, doi: 10.1109/ACCESS.2016.2601145.
[34] A. Sam, J. Wiart, L. Martens, and W. Joseph, "Assessment of long-term spatio-temporal radiofrequency electromagnetic field exposure," *Environ. Res.*, vol. 161, pp. 136–143, 2028.
[35] S. Aerts et al., "In situ assessment of 5G NR massive MIMO base station exposure in a commercial network in Bern, Switzerland," *Appl. Sci.*, vol. 11, no. 8, p. 3592, 2021.
[36] S. Aerts et al., "In-situ measurement methodology for the assessment of 5G NR massive MIMO base station exposure at sub-6 GHz frequencies," *IEEE Access*, vol. 7, pp. 184658–184667, 2019, doi: 10.1109/ACCESS.2019.2961225.
[37] M. S. Elbasheir, R. A. Saeed, and S. Edam, "Electromagnetic field exposure boundary analysis at the near field for multi-technology cellular base station site," *Inst. Eng. Technol. Commun.*, vol. 18, no. 1, pp. 11–27, 2024.
[38] M. S. Elbasheir, R. A. Saeed, and S. Edam, "Measurement and simulation-based exposure assessment at a far-field for a multi-technology cellular site up to 5G NR," *IEEE Access*, vol. 10, pp. 56888–56900, 2022, doi: 10.1109/ACCESS.2022.3177732.
[39] *Case Studies Supporting*, IEC Standard 62232 ed2 106/463/cd, Sep. 2018.
[40] B. Thors, A. Furuskär, D. Colombi, and C. Törnevik, "Time-averaged realistic maximum power levels for the assessment of radio frequency exposure for 5G radio base stations using massive MIMO," *IEEE Access*, vol. 5, pp. 19711–19719, 2017, doi: 10.1109/ACCESS.2017.275345.
[41] P. Baracca, A. Weber, T. Wild, and C. Grangeat, "A statistical approach for RF exposure compliance boundary assessment in massive MIMO systems," in *Proc. 22nd Int. ITG Workshop Smart Antennas (WSA)*, 2018, pp. 1–6.
[42] A.-K. Lee, S.-B. Jeon, and H.-D. Choi, "EMF levels in 5G New radio environment in Seoul, South Korea," *IEEE Access*, vol. 9, pp. 19716–19722, 2021, doi: 10.1109/ACCESS.2021.3054363.
[43] T. Rumeng, S. Ying, W. Tong, and Z. Wentao, "Electromagnetic field safety compliance assessments for 5G wireless networks," in *Proc. IEEE Int. Symp. Electromag. Compat. Signal/Power Integrity (EMCSI)*, 2020, pp. 659–662, doi: 10.1109/EMCSI38923.2020.9191518.
[44] A. Jain and P. Tupe-Waghmare, "Radiation measurements at repeated intervals for various locations of SIU campus and calculation of compliance distance from a cell tower," in *Proc. Int. Conf. Autom. Control Dyn. Optim. Techn. (ICACDOT)*, 2016, pp. 804–808, doi: 10.1109/ICACDOT.2016.7877698.
[45] "SRM-3006 EMF selective safety test solutions." Narda. 2022. [Online]. Available: https://www.narda-sts.com/en/selective-emf/srm-3006-field-strength-analyzer/
[46] "Infovista." 2021. [Online]. Available: https://www.infovista.com/tems/investigation
[47] "Mapbis." 2024. [Online]. Available: https://mapbis.com/mapinfo-pro/

MOHAMMED S. ELBASHEIR (Senior Member, IEEE) received the B.Sc. and M.Sc. degrees in communication engineering from the University of Khartoum, Sudan. He is currently pursuing the Ph.D. degree in wireless communication with the School of Electronic Engineering, Sudan University of Science and Technology. From 1998 to 2005, he worked as a Planning and Optimization Engineer with Etisalat Corporation, UAE. Since 2006, he has been working as the Senior Director of Mobile Network Planning and Design with Etihad Etisalat Company (Mobily), Saudi Arabia. His major role is planning and deploying modern mobile technologies, such as 4G, 5G, and IoT. He has published a group of research articles and papers in IEEE.

RASHID A. SAEED (Senior Member, IEEE) received the Ph.D. degree in communications and network engineering from Universiti Putra Malaysia. He is currently a Professor with the Computer Engineering Department, Taif University, Saudi Arabia. He is also working with the School of Electronics Engineering, Sudan University of Science and Technology. He was a Senior Researcher with Telekom Malaysia^{TM} Research and Development and MIMOS. He published more than 150 research papers, books, and book chapters on wireless communications and networking in peer-reviewed academic journals and conferences. He supervised more than 50 M.Sc./Ph.D. students. His areas of research interest include computer networks, cognitive computing, computer engineering, wireless broadband, and WiMAX Femtocell. He is successfully awarded three U.S patents in these areas. He is a member of IEM, SigmaXi, and SEC.

SALAHELDIN EDAM received the B.Sc. degree in electronics engineering from the Sudan University of Science and Technology (SUST), the Post Graduate Diploma (APGD) degree in advanced information technology (advanced networking and telecommunication), the M.Sc. degree in information technology (computer network systems) from SUST, and the Ph.D. degree in communications and information systems from the Beijing University of Posts and Telecommunications. He was an Engineer with Sudan Telecommunication Company. He is currently an Assistant Professor with the School of Electronics Engineering, SUST. He has published many research papers in journals and conferences. He supervised many M.Sc. students in addition to co-supervisor for many Ph.D. students. His areas of research interest include wireless communications, software-defined networking, IoT, and computer network systems.